Journal of Molecular Neuroscience

ISSN0895-8696/07/31:47–58/$30.00
JMN (Online)ISSN 1558-6804
DOI 10.1385/JMN/31:01:47

ORIGINAL ARTICLE

Distribution of Histone Deacetylases 1–11 in the Rat Brain

Ron S. Broide,[1] Jeff M. Redwine,[1] Najla Aftahi,[1] Warren Young,[1] Floyd E. Bloom,[1] and Christopher J. Winrow*,[2]

[1]Neurome, La Jolla, CA 92037; and [2]Merck Research Laboratories, West Point, PA 19486

Received May 15, 2006; Accepted June 3, 2006

Abstract

Although protein phosphorylation has been characterized more extensively, modulation of the acetylation state of signaling molecules is now being recognized as a key means of signal transduction. The enzymes responsible for mediating these changes include histone acetyl transferases and histone deacetylases (*HDAC*s). Members of the *HDAC* family of enzymes have been identified as potential therapeutic targets for diseases ranging from cancer to ischemia and neurodegeneration. We initiated a project to conduct comprehensive gene expression mapping of the 11 *HDAC* isoforms (*HDAC1–11*) (classes I, II, and IV) throughout the rat brain using high-resolution *in situ* hybridization (ISH) and imaging technology. Internal and external data bases were employed to identify the appropriate rat sequence information for probe selection. In addition, immunohistochemistry was performed on these samples to separately examine *HDAC* expression in neurons, astrocytes, oligodendrocytes, and endothelial cells in the CNS. This double-labeling approach enabled the identification of specific cell types in which the individual *HDAC*s were expressed. The signals obtained by ISH were compared to radiolabeled standards and thereby enabled semiquantitative analysis of individual *HDAC* isoforms and defined relative levels of gene expression in >50 brain regions. This project produced an extensive atlas of 11 *HDAC* isoforms throughout the rat brain, including cell type localization, providing a valuable resource for examining the roles of specific HDACs in the brain and the development of future modulators of *HDAC* activity.

DOI 10.1385/JMN/31:01:47

Index Entries: Histone deacetylase; gene expression; brain; transcription.

Introduction

Chromatin remodeling by modulation of histone acetylation states is carried out by histone deacetylases (*HDAC*s) and histone acetyl transferases (*HAT*s) in association with multiprotein complexes (for review, *see* Marks et al., 2003; Shabbeer and Carducci, 2005). In addition to regulating transcription through modifying the acetylation state of histones, acetylation is being recognized as an important post-translational modification for many nonhistone proteins (Bereshchenko et al., 2002; Haggarty et al., 2003; Vaghefi and Neet, 2004). The critical roles of the *HDAC* and HAT family members in transcription and signal transduction are quickly emerging. In a similar manner, the contribution of aberrant acetylation in a host of disease states is being recognized. The role of *HDAC*s and their increased or decreased activities have been implicated in multiple indications, including cancer (Choi et al., 2001; Richon et al., 2001; Johnstone, 2002), cardiovascular disease (Ito et al., 2005; Lin, 2005), asthma (Ito et al., 2002; Choi et al., 2005), and other disease states (Chiurazzi et al., 1999; Alarcon et al., 2004). By far, the most attention has been focused on the use of *HDAC* modulators for cancer, with several late-stage clinical trials ongoing (for review, *see* Marks et al., 2004; Acharya et al., 2005; Kelly et al., 2005; Moradei et al., 2005). The application

*Author to whom all correspondence and reprint requests should be addressed. E-mail: christopher_winrow@merck.com

of *HDAC* modulators for CNS indications has not been investigated as heavily; however, indications of *HDAC* dysregulation in disorders such as Huntington's disease (Hoshino et al., 2003; Gardian et al., 2005), ischemia (Ren et al., 2004), Parkinson's disease (Kawaguchi et al., 2003), and roles in neurogenesis, neuroprotection, and neurodegeneration have been described recently (Jeong et al., 2003; Hao et al., 2004; Panteleeva et al., 2004; Langley et al., 2005; Saha and Pahan, 2005; Yamaguchi et al., 2005). Modulation of *HDAC* activity has been the focus of much recent attention, along with the realization that acetylation is a significant factor in regulating transcriptional activity of genes involved in a number of physiologic and pathological states.

The HDACs have been classified into four classes, based on localization and amino acid sequence similarities. Class-I *HDAC*s (*HDAC1*, *-2*, *-3*, and *-8*) are localized in the nucleus. Class-II *HDAC*s (*HDAC4–7*, *-9*, and *-10*) shuttle between the cytoplasm and nucleus and, like class-I HDACs, require Zn for catalytic activity. Class-III *HDAC*s (*SIRT1–7*) are Zn-independent and nicotinamide adenine dinucleotide (NAD)-dependent enzymes similar to yeast Sir2 proteins. Histone deacetylase 11 (*HDAC11*) shares characteristics of class-I and -II *HDAC*s but is considered a class-IV *HDAC* based on potentially distinct physiological roles (for review, *see* Roth et al., 2001; Gregoretti et al., 2004; Shabbeer and Carducci, 2005). Interestingly, although there is similarity in the catalytic domains, recent experiments have shown that there might be little functional overlap between the *HDAC*s (Robyr et al., 2002). Previous studies have described general localization of some *HDAC*s; however, a detailed analysis of *HDAC* expression patterns in the CNS has not been performed.

Given the large number of *HDAC* isoforms and diversity of substrates, a better understanding of the localization of *HDAC*s is clearly warranted. Previous information on *HDAC* distribution has been limited to global analysis of tissues by Northern blotting, RT-PCR, and some *in situ* hybridization (ISH) of specific regions. The present study offers the first comprehensive fine mapping of *HDAC* mRNA expression throughout the brain. This approach enabled direct comparison between *HDAC* isoforms by including radiolabeled standards along with each slide. By incorporating this information, we were able to analyze the relative mRNA expression levels of *HDAC* isoforms to each other. This study is the first extensive characterization of the 11 *HDAC*s in the CNS, showing the heterogeneity of *HDAC* expression patterns through >50 brain regions and demonstrating that although *HDAC*s are expressed primarily in neurons, a subset is also found in oligodendrocytes. In addition to the biological significance of this expression atlas, these data serve as a valuable tool for the development of *HDAC* therapeutics for CNS diseases.

Materials and Methods

Tissue Preparation

Male rats ($n = 3$) were anesthetized with approx 300 mg/kg avertin (Sigma, St. Louis, MO) and perfused transcardially with 15 mL of saline at room temperature (RT), followed by 100 mL of 4% paraformaldehyde (PFA) at 4°C. Brains were then dissected, postfixed in 4% PFA for 1 h. at 4°C, transferred to 15% sucrose at 4°C overnight, transferred to 30% sucrose overnight at 4°C, frozen on dry ice, and stored at –80°C. Coronal brain sections (20 µm thick) were cut by cryostat, thaw mounted onto poly-L-lysine-coated slides, and stored at –80°C until use. A 1-in-100 series of sections was used for each animal per gene. All procedures on these animals were in accordance with established guidelines and were reviewed and approved by the Institutional Animal Care and Use Committee (IACUC).

ISH

Ten 40-mer oligonucleotides were chosen (Invitrogen, Carlsbad, CA) for each HDAC isoform and were labeled by 3′ tailing with [^{35}S]dATP (>1000Ci/mmol) (Amersham Biosciences, Piscataway, NJ) for radioactive ISH or DIG-dUTP (Roche) for fluorescence ISH; ISH was performed as described previously (Broide et al., 2004). Briefly, slide-mounted brain sections were pretreated with 1 mg/mL proteinase K, and incubated for 18 h at 42°C with hybridization solution containing either [^{35}S]dATP-labeled or DIG-labeled oligoprobes. Adjacent sections were incubated with the labeled oligoprobe plus 1000-fold excess concentration of unlabeled probe to determine the nonspecific hybridization signal. Following hybridization, sections were washed in decreasing salinity (2.0–0.1 × SSC with 1 m*M* DTT) for 30 min each at 42°C. For fluorescence ISH, sections were blocked and then incubated with anti-DIG primary antibody (Roche), followed by a biotinylated secondary antibody (Vector labs), alkaline phosphatase–conjugated strepavidin, and finally with ELF 97 phosphatase substrate (Invitrogen) for 60 min. For radioactive ISH, brain sections were

dehydrated, dried in a stream of cold air, and exposed to Biomax-MR film (Kodak) for 6–8 d, along with ^{14}C-labeled calibration standards at 4°C. The radioactive standards, comprising an 11-point scale, were designed to encompass the sensitivity limits of the film. Film was developed, and slides were emulsion dipped (Kodak). Following 18–25 d of exposure, slides were developed, and the slide-mounted sections were counterstained with cresyl violet and thionine, and coverslipped.

Double-Labeling Fluorescence ISH and Immunohistochemistry

For double-labeling studies to identify cell phenotypes, mouse anti-*NeuN* (Chemicon, 1:100) was used to label neurons, mouse anti-*APC* (Ab-7) (Calbiochem, 1:100) was used to label mature oligodendrocytes, rabbit anti-*GFAP* (DakoCytomation, 1:100) was used to label astrocytes, rabbit anti-Von Willibrand factor (Chemicon, 1:50) was used to label vessel endothelial cells, and mouse anti-*CD11*b/c (BD Biosciences Pharmingen, 1:100) was used to label microglia. After postfixation in 4% PFA, brain sections were placed in blocking buffer for 1 h, followed by incubation with the cell phenotype–specific primary antibody (as above) overnight at RT. Slides were then incubated with appropriate species-matched secondary antibodies (goat anti-mouse or goat anti-rabbit, 1:100) conjugated to Alexa Fluor 546 (Invitrogen, 20 μg/ml diluted 1:100). After washing, sections were counterstained with DAPI, coverslipped with Prolong Gold (Invitrogen), and stored at 4°C in the dark.

Data Analysis

Qualitative analysis of relative hybridization signal intensity for each *HDAC* isoform was performed on autoradiographic images. More than 50 individual brain regions were examined and scored on a scale of low to high (0–5) intensity. For each brain region, the signal intensity between the different isoforms was compared in relation to the radioactive standards on each film. Global expression levels were calculated as the sum of regional expression values, and an overall rank order of expression was generated. Double-labeling ISH/immunohistochemical analysis was performed for each *HDAC* isoform in association with the different cell markers. Criteria for positively double-labeled cells involved the presence of specific ELF labeling (green), along with cell type–specific labeling (red), and the presence of a DAPI-labeled nucleus (blue).

Results

HDAC 1–11 *Show Overlapping and Distinct Regional and Cell Layer–Specific Expression*

To examine the patterns of expression of the 11 *HDAC* isoforms throughout the brain, a project was initiated using technology developed by Neurome (Broide et al., 2004). Both internal and external data base information was used to design multiple oligonucleotide probes for each *HDAC* isoform (Fig. 1; *see below,* Supplemental Methods: Data Analysis). High-resolution ISH was performed using methods described previously (Broide et al., 2004). Interestingly, the *HDAC* isoforms showed both overlapping and distinct patterns of expression throughout the rat brain (Fig. 2). Relative levels of each *HDAC* transcript could be determined, as internal labeling controls were employed for each set of slides (Fig. 2). Representative coronal sections at the level of bregma –3.1 are shown in Fig. 2, demonstrating the unique patterns of expression and the varying intensities of each *HDAC* isoform (Franklin and Paxinos, 1997). In these sections it can be seen readily that *HDAC11*, *-5*, and *-3* are the most highly expressed isoforms globally, particularly in the cortical regions.

For each *HDAC* isoform, sections were analyzed throughout the brain and data were compiled from at least three separate animals (Fig. 3). Adjacent control sections showed background levels of hybridization. As shown in Table 1, qualitative analysis of signal intensity for each *HDAC* isoform was performed for >50 brain regions and scored from low to high (0–5) throughout the brain. Global expression levels were calculated as the sum of regional expression values, with the rank order of expression listed below. The global rank order shows that *HDAC11*, *-3*, and *-5* are expressed most highly, and *HDAC10*, *-9*, and *-7* have the lowest expression levels throughout the brain. The only regions with substantial *HDAC10* expression are the CA1, CA3, and dentate gyrus. Representative images of *HDAC11* expression from 10 rostrocaudal sections are presented in Fig. 3. At this level of resolution, the regional expression patterns can be seen clearly and the qualitative expression in >50 regions is listed in Table 1. At higher magnification the expression patterns of the individual *HDAC*s can be viewed at the level of subregions and cell layers. This is illustrated in Fig. 4, where the expressions of *HDAC3* and *HDAC11* are compared in the same coronal brain regions. In the top panels, expression in the cerebellar regions is observed. At higher magnification (middle

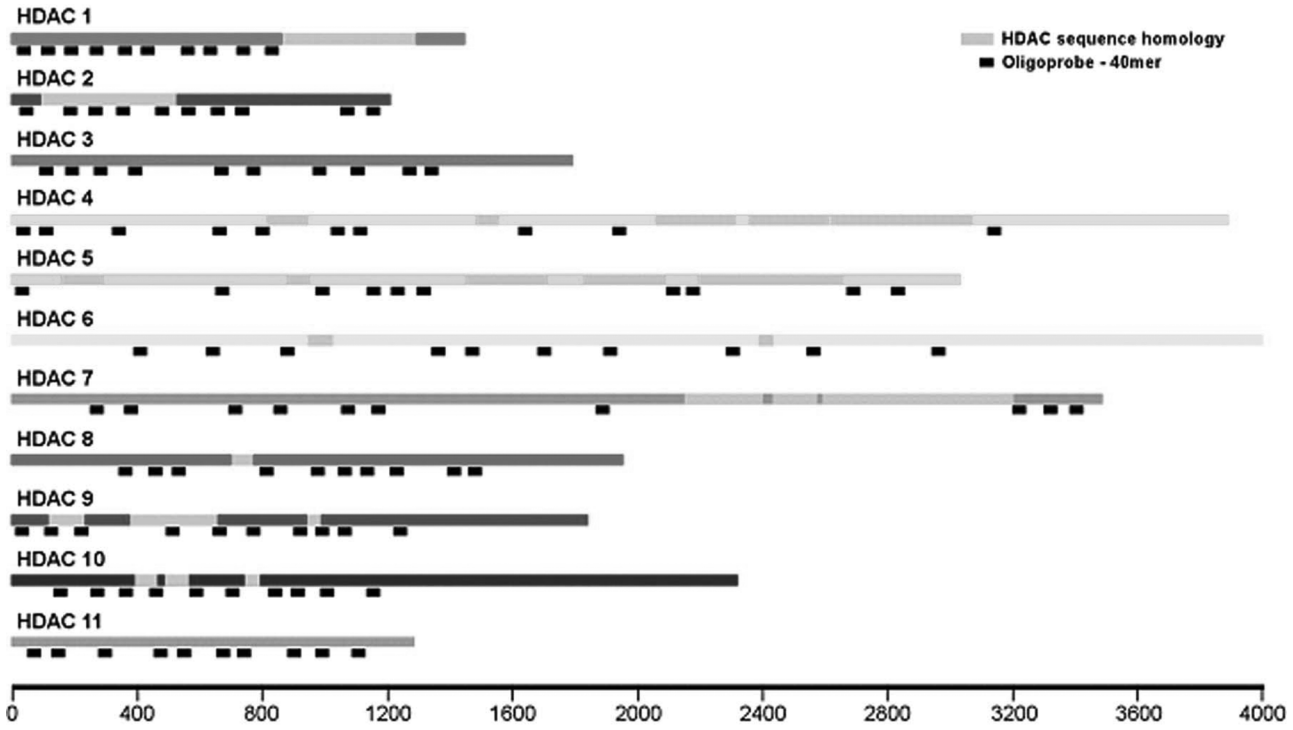

Fig. 1. Oligonucleotide probes designed for ISH of *HDAC1–11*. Ten 40-mer oligonucleotides were selected for each *HDAC* isoform. Rat *HDAC* sequence information was obtained from internal and public data bases and was used to design the probes. Gray shading indicates regions of sequence homology between the *HDAC*s, and black regions below the sequences indicate the location of individual probes. The size of each transcript is shown on the *x*-axis (bp).

panels), *HDAC3* is observed to be highly expressed in cerebellar granule cells, whereas *HDAC11* is expressed not only in the granule cell layer but also in the Purkinje cell layer. Of all *HDAC* genes examined, only *HDAC11* was found to be expressed in the Purkinje cell layer. The lower panel shows that both *HDAC3* and *HDAC11* are expressed in the hippocampus, but the resolution of these images shows clearly the unique expression of *HDAC11* in CA1, with lower expression in CA3 and dentate gyrus. This is an expression pattern rarely observed in the hippocampus. Similar analyses at high magnification were performed for all 11 *HDAC*s throughout the rat brain, and the data are shown in Table 1.

HDAC *Isoforms Are Expressed Primarily in Neurons, with a Subset Also Found in Oligodendrocytes*

Double labeling was performed to identify the cell types in which the *HDAC*s were expressed. Sections were stained with labeled oligonucleotide probes for the individual *HDAC* isoforms and by immunohistochemistry for selected cell type markers. Antibodies were used to identify neurons (anti-*NeuN*), oligodendrocytes (anti-*APC*), astrocytes (anti-*GFAP*), and vessel endothelial cells (anti-Von Willibrand factor). Anti-*CD11*b/c was used to label microglia; however, microglial labeling was not significantly above background and double labeling was not observed (data not shown). Sample images are shown in Fig. 5, and a summary of the results is presented in Table 2. Low signal from some *HDAC* isoforms precluded cell type identification; however, most *HDAC*s were found to be expressed primarily in neurons (Fig. 5; Table 2). A subset (*HDAC2–5* and *-11*) was also expressed in oligodendrocytes. No colocalization of *HDAC*s was observed in astrocytes or vessel endothelial cells (Fig. 5; Table 2). Overall, these studies show that in the rat CNS the *HDAC*s are expressed primarily in neurons, with some isoform-specific expression in oligodendrocytes.

Discussion

In the current study we generated a comprehensive mRNA expression atlas of the 11 *HDAC*s in rat brain and identified which cell types expressed these genes. Because of the resolution of the images and

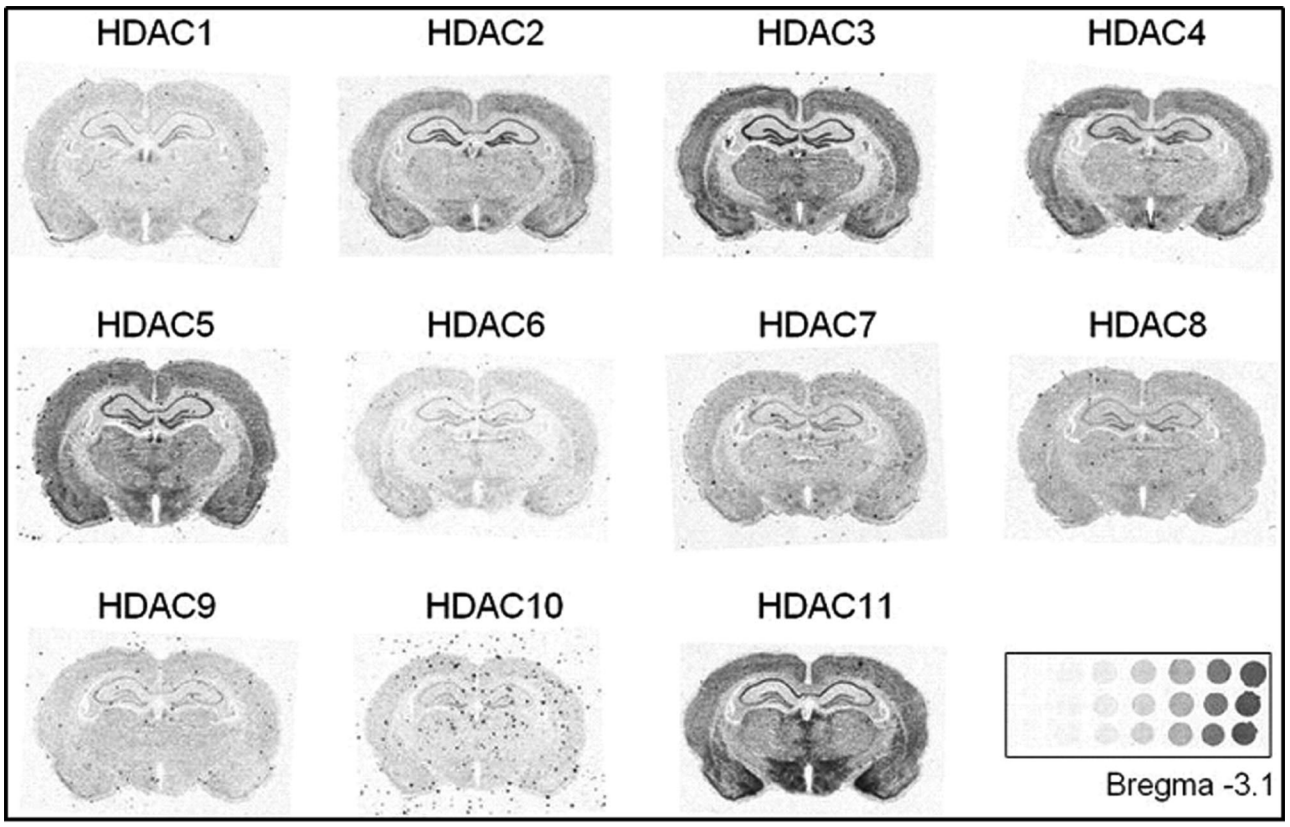

Fig. 2. *ISH* shows distinct expression differences between *HDAC* isoforms in the rat brain. Representative autoradiographic images of the same brain region (Bregma –3.1) for the 11 *HDAC* isoforms are shown. Sections (20 μm) were obtained, and a 1-in-100 series of sections was used for each animal per gene. At least three separate animals were examined for each *HDAC* isoform. Adjacent control sections showed background levels of hybridization (data not shown). The reference standards are shown in the lower right panel, enabling comparison of relative intensity between standards and isoforms.

the method in which the experiments was performed, these data can be further analyzed quantitatively or examined in greater detail to focus on more restricted regions of interest. In addition, this information might be used to assign previously unknown roles to individual *HDAC* isoforms, given their anatomical and cellular locations. For example, the presence of *HDAC2–5* and *-11* in oligodendrocytes might suggest a role in myelination or other processes that could be better understood in the context of pathological conditions such as multiple sclerosis. The observation that only *HDAC1*, *-3*, and *-5* are expressed in choroid plexus might suggest involvement in developmental processes and cerebral spinal fluid regulation (Emerich et al., 2005). One of the most interesting findings was the distribution of *HDAC11*. Recently identified as the only member of the class-IV *HDAC*s (Gao et al., 2002), *HDAC11* has not been characterized extensively beyond genomic localization (Voelter-Mahlknecht et al., 2005). Histone deacetylase 11 (*HDAC11*) activity has been linked to cancers and shows an interesting response to *HDAC* inhibitors in the context of acute myeloid leukemia (Bradbury et al., 2005). The data generated from our studies is a prime example of how this approach could identify new roles for *HDAC11*. For example, the unusual expression pattern of *HDAC11* in hippocampus suggests a possible role in learning and memory, whereas the high level of expression selectively in the Purkinje cell layer might suggest a role in locomotor activity and ataxic syndromes.

Previous investigations of small subsets or individual *HDAC*s agree well with our studies. Work by Shen et al. (2005) described a role for *HDAC3* in myelination during rat CNS development, and our data show that *HDAC3* is one of the few isoforms expressed in oligodendrocytes. In a model of Huntington's disease, *HDAC3* activity was observed in striatum (Gardian et al., 2005), where we also noted strong expression of *HDAC3* mRNA. Histone

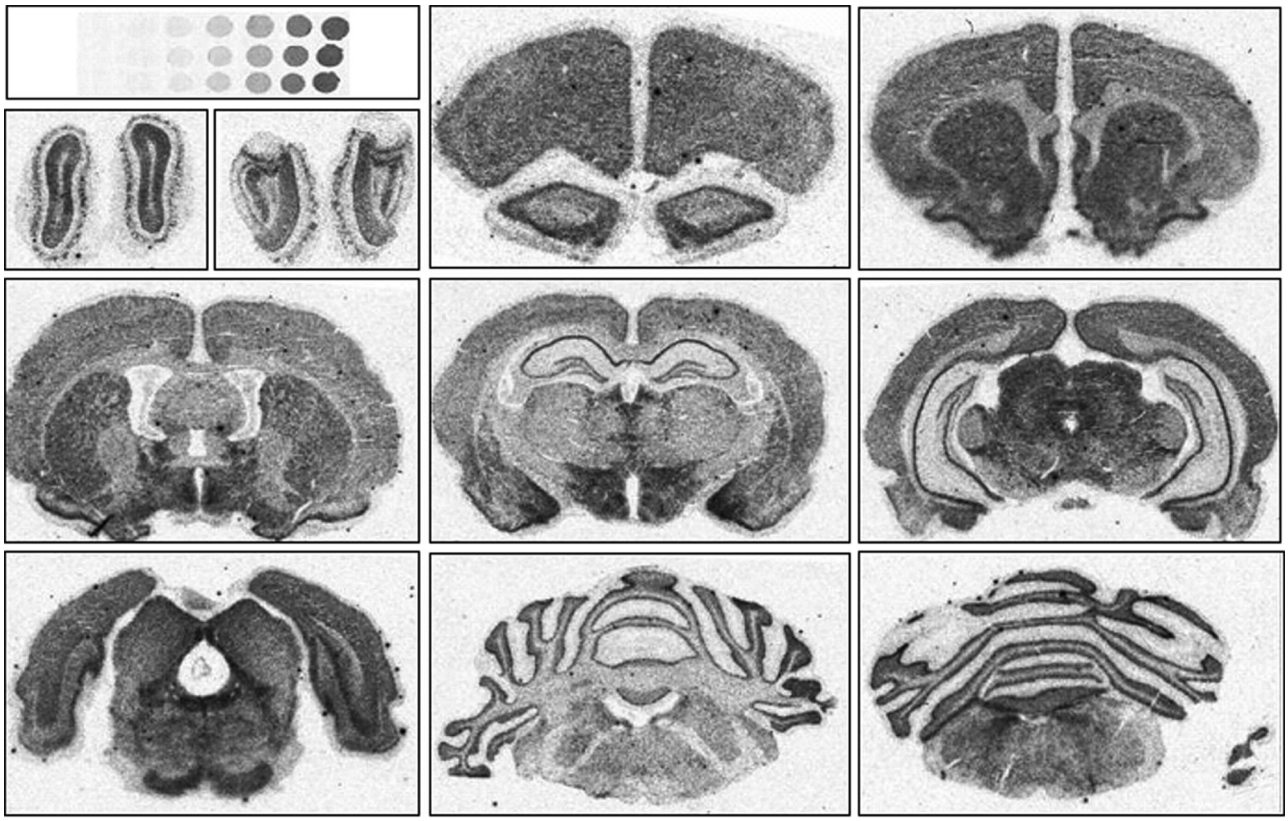

Fig. 3. Distinct patterns of regional expression for *HDAC11* throughout the rat brain. Representative autoradiographic images showing the detailed localization of *HDAC11* across 10 separate brain sections. The reference standards are shown in the upper left panel enabling comparison of relative intensity between standards and isoforms.

deacetylase 4 (*HDAC4*) recently was found to be involved in mediating neuronal apoptosis in cerebellar granule neurons (Bolger and Yao, 2005), which is the region where *HDAC4* is expressed most highly in our experiments. In studies of Huntington's disease, *HDAC5* expression was localized to cortical neurons (Hoshino et al., 2003), which is where we also observed high levels of *HDAC5* mRNA expression.

Most current *HDAC* inhibitors have broad specificity, inhibiting multiple *HDAC* isoforms. This might actually serve as a benefit for some of the current indications, such as cancer in which inhibition of several *HDAC*s could slow growth or promote apoptosis (for review, *see* Dokmanovic and Marks, 2005). However, in many cases, the contribution of individual *HDAC*s is not known. Several studies have also employed nonselective *HDAC* inhibitors to demonstrate an effect in models of CNS diseases. Trichostatin A is a broad *HDAC* inhibitor shown to be efficacious in a mouse experimental allergic encephalomyelitis model of multiple sclerosis (Camelo et al., 2005). In an MPTP model of Parkinson's disease, phenylbutyrate demonstrated improvement in outcome (Gardian et al., 2004). Trichostatin A was also shown to affect acetylation and alter circadian-regulated gene expression (Naruse et al., 2004). In addition to applications for cancer, vorinostat (suberoylanilide hydroxamic acid) and other *HDAC* inhibitors are being evaluated for their ability to benefit the transcriptional deficits in Huntington's disease (Richon et al., 2001; Kouraklis and Theocharis, 2002; Ferrante et al., 2003; Hockly et al., 2003; Alarcon et al., 2004). Although targeting multiple *HDAC* isoforms might be important for certain indications and proof-of-concept studies, the development of more selective compounds could prove beneficial by reducing off-target activity and significantly contributing to our understanding of the biological roles of *HDAC*s in the CNS. One goal of this type of approach is the selective modulation of a particular *HDAC*, or subset of *HDAC*s, that is proposed to be involved in the disease state. In this scenario, it is important to understand where and in what cells individual *HDAC*s are expressed. This is particularly

Table 1
Regional Expression of *HDAC1–11* in Rat Brain

Brain Region	HDAC1	HDAC2	HDAC3	HDAC4	HDAC5	HDAC6	HDAC7	HDAC8	HDAC9	HDAC10	HDAC11
Olfactory bulb											
Glomerular layer	2.0	2.0	4.0	4.0	4.0	1.0	0.5	0.5	0.0	0.0	4.0
Granular cell layer	3.0	5.0	5.0	5.0	5.0	2.0	1.5	2.0	1.0	0.5	5.0
Anterior olfactory nucleus	2.0	3.0	3.5	3.0	3.5	1.0	1.0	0.5	0.5	0.0	4.0
Olfactory tubercle	1.0	3.5	4.0	2.0	3.5	1.0	1.0	0.5	0.5	0.0	5.0
Tenia tecta-dorsal	2.0	4.0	5.0	4.0	3.0	1.5	1.0	0.5	0.0	0.0	4.0
Cortex											
Frontal/Orbital cortex	2.0	3.0	3.5	3.5	3.5	1.0	0.5	0.0	0.5	0.5	4.0
Motor cortex	2.0	3.0	3.5	3.5	3.5	1.0	0.5	0.0	0.5	0.5	4.0
Parital/somatosensory cortex	2.0	3.0	3.5	3.5	3.5	1.0	0.5	0.0	0.5	0.5	4.0
Insular cortex	2.0	3.0	3.5	3.5	3.5	1.0	0.5	0.0	0.5	0.5	4.0
Cingulate/retrosplenial cortex	2.0	3.0	3.5	3.5	3.5	1.0	0.5	1.0	0.5	0.5	4.0
Auditory cortex	2.0	3.0	3.5	3.5	3.5	1.0	0.5	0.5	0.5	0.5	4.0
Perirhinal cortex	2.0	3.0	3.5	3.5	3.5	1.0	0.5	0.5	0.5	0.5	4.0
Visual cortex	2.0	3.0	3.5	3.5	3.5	1.0	0.5	1.0	0.5	0.5	4.0
Ectorhinal cortex	2.0	3.0	3.5	3.5	3.5	1.0	0.5	0.0	0.5	0.5	4.0
Entorhinal cortex	2.0	3.0	3.5	3.5	3.5	1.0	0.5	0.0	0.5	0.5	4.5
Piriform cortex	3.0	4.0	5.0	4.0	4.0	1.5	1.5	1.0	1.0	0.5	5.0
Caudate putamen	0.5	2.0	3.0	1.0	3.0	0.5	0.5	0.0	0.0	0.0	4.0
Nucleus accumbens	0.5	2.0	3.0	1.0	3.0	0.5	0.5	0.0	0.0	0.0	4.0
Globus palidus	0.0	0.0	1.0	0.5	1.0	0.0	0.0	0.0	0.0	0.0	2.0
BNST	1.0	2.0	3.0	2.0	3.0	0.5	0.5	0.0	0.0	0.0	5.0
Septum	0.5	1.5	2.5	1.5	2.5	0.5	0.5	0.0	0.0	0.0	3.5
Amygdala	2.5	3.0	3.5	3.0	3.0	1.0	1.0	1.0	0.5	0.5	4.5
Hippocampus											
CA1 pyramidal layer	2.5	4.5	5.0	4.5	5.0	2.0	1.0	2.0	1.0	1.0	5.0
CA3 pyramidal layer	2.5	4.5	5.0	4.5	5.0	2.0	1.0	2.0	1.0	1.0	4.0
DG granular layer	3.5	4.5	5.0	4.5	5.0	2.0	1.0	3.0	1.0	1.0	3.0
Molecular layer	0.0	0.0	0.0	0.0	0.0	0.0	0.0	0.0	0.0	0.0	0.0
Choroid plexus	2.0	0.0	3.0	0.0	2.0	0.0	0.0	0.0	0.0	0.0	0.0
Thalamus / Midbrain											
Medial habenula	3.0	3.0	4.0	3.0	5.0	1.5	1.0	1.5	1.0	0.5	4.5
Paraventricular nucleus	0.5	1.0	2.5	1.0	3.0	0.5	0.0	0.0	0.0	0.0	4.5
Central medial nucleus	0.5	1.0	2.5	1.5	3.0	0.5	0.5	0.0	0.0	0.0	4.5
Ventral tegmental area	1.0	1.5	2.5	2.0	2.5	0.5	0.0	0.5	0.5	0.0	4.0
Substantia nigra-compacta	1.0	1.5	3.5	2.5	3.5	1.0	1.0	1.0	1.0	0.0	4.0
Substantia nigra-reticulata	0.5	1.0	1.5	1.0	1.5	0.0	0.0	0.0	0.0	0.0	3.0
Hypothalamus											
Medial preoptic nucleus	1.5	2.0	3.5	2.5	3.5	1.0	0.5	1.0	0.0	0.0	5.0
Lateral preoptic nucleus	1.0	1.5	3.0	2.0	3.0	0.5	0.0	0.5	0.0	0.0	4.5
Paraventricular nucleus	1.0	1.5	3.0	2.0	3.0	0.5	0.5	0.5	0.0	0.0	4.5
Periventricular nucleus	1.0	1.0	3.0	5.0	2.5	0.5	0.0	0.5	0.0	0.0	4.0
Dorsomedial nucleus	1.5	1.5	3.5	2.5	3.5	1.0	0.5	0.5	0.0	0.0	5.0
Ventromedial hyp. Nucleus	2.0	2.5	3.5	2.5	3.5	1.0	0.5	1.0	0.0	0.0	5.0
Zona incerta	1.5	1.5	3.5	2.5	3.5	1.0	0.5	1.0	0.0	0.0	5.0
Pons											
Pontine nucleus	2.0	3.0	3.5	3.5	3.5	1.0	0.5	1.0	0.5	0.5	4.0
Dorsal raphe nucleus	1.5	2.0	3.0	2.5	3.0	1.0	0.5	0.5	0.5	0.0	5.0
Interpeduncluar nucleus	1.0	1.5	2.5	2.0	3.0	0.5	0.5	0.5	0.0	0.0	4.0
Pendunculopontine nucleus	1.0	1.5	2.0	2.0	2.0	0.5	0.0	0.0	0.0	0.0	5.0
Periaqueductal gray	0.5	1.5	2.0	2.5	2.0	1.0	0.5	0.5	0.5	0.0	5.0
Superior colliculus	1.0	1.0	2.0	2.0	2.0	0.5	0.0	0.0	0.0	0.0	4.5
Inferior colliculus	1.0	1.0	2.0	2.0	2.0	0.5	0.0	0.0	0.0	0.0	4.0
Cerebellum											
Granule cell layer	4.0	4.0	5.0	5.0	5.0	1.5	1.5	2.0	0.5	0.0	4.0
Molecular layer	0.0	0.0	0.0	0.5	0.0	0.0	0.0	0.0	0.0	0.0	0.0
Purkinje cell layer	0.0	0.0	0.0	0.0	0.0	0.0	0.0	0.0	0.0	0.0	5.0
Medulla											
Principal sensory nucleus	0.5	1.5	2.0	2.0	2.0	0.5	0.5	0.5	0.0	0.0	3.0
Reticular nuclei	0.5	1.5	1.5	1.5	1.5	0.5	0.5	0.5	0.0	0.0	2.5
Locus coeruleus	1.0	3.0	4.0	3.0	4.0	1.5	1.0	0.5	0.0	0.0	4.0
Solitary nucleus	1.0	2.0	3.0	2.0	3.0	0.5	0.5	1.0	0.0	0.0	5.0
Facial nucleus	0.5	2.0	4.0	2.0	4.0	0.5	0.5	1.5	0.0	0.0	3.0
Spinal cord	1.0	2.0	2.5	2.0	2.5	0.5	0.5	0.5	0.0	0.0	3.5
SUM	**81.0**	**123.5**	**174.0**	**144.0**	**171.0**	**47.0**	**29.5**	**33.0**	**16.0**	**10.5**	**221.5**
Rank Order	**6**	**5**	**2**	**4**	**3**	**7**	**9**	**8**	**10**	**11**	**1**

Qualitative analysis of signal intensity for each *HDAC* isoform was performed for the >50 brain regions listed and scored from low to high (0–5). Global expression levels were calculated as the sum of regional expression values, with the rank order of expression listed below. Data were compiled from at least three separate animals for each *HDAC* isoform.

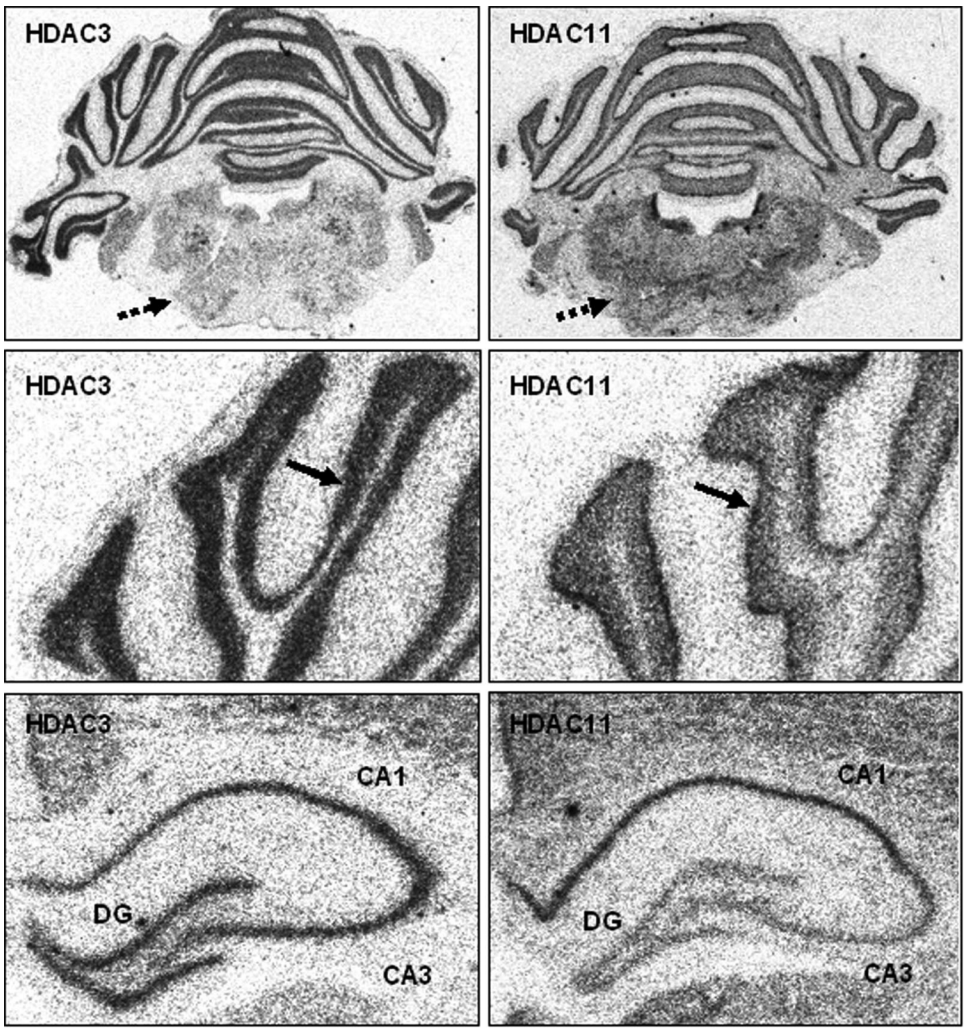

Fig. 4. High-resolution images show regional and cell-layer-specific expression differences between *HDAC3* and *HDAC11*. Top panels: At low magnification, expression of *HDAC11* mRNA is clearly observed in the medulla (broken arrow), compared with much lower expression of *HDAC3* mRNA within the same regions. Middle panels: At higher resolution, *HDAC3* mRNA is highly expressed in the granule cell layer of the cerebellum (arrow), whereas *HDAC11* is expressed more highly in the Purkinje cell layer and to a lesser extent in the granule cell layer. Bottom panels: *HDAC11* mRNA is expressed more highly in the CA1 region and less in the CA3 and dentate gyrus (DG) regions.

important for developing *HDAC* modulators for neurological diseases. Toward this end, a better understanding of *HDAC* expression in the CNS clearly would be of use. The data that we have presented enables the identification of specific regional expression patterns that indicate which isoforms might be of most interest for targeting in CNS indications. As described above, one of the major hurdles faced by this field is the availability of subtype-selective *HDAC* inhibitors. It will be important to further examine the roles of individual isoforms as more selective *HDAC* inhibitors become available and through the use of genetic models. Although rapid advances are being made in this area, an understanding of the localization of these isoforms is critical in identifying potential indications for *HDAC* modulators. Even in the absence of truly selective compounds, the information from this study could help the selection of appropriate agents for testing in disease models. For example, the observation that *HDAC11* is the only isoform expressed in the Purkinje cell layer of the cerebellum might suggest that studies of *HDAC* modulators for ataxia should consider available compounds that alter *HDAC11* activity, even though they might modulate other isoforms.

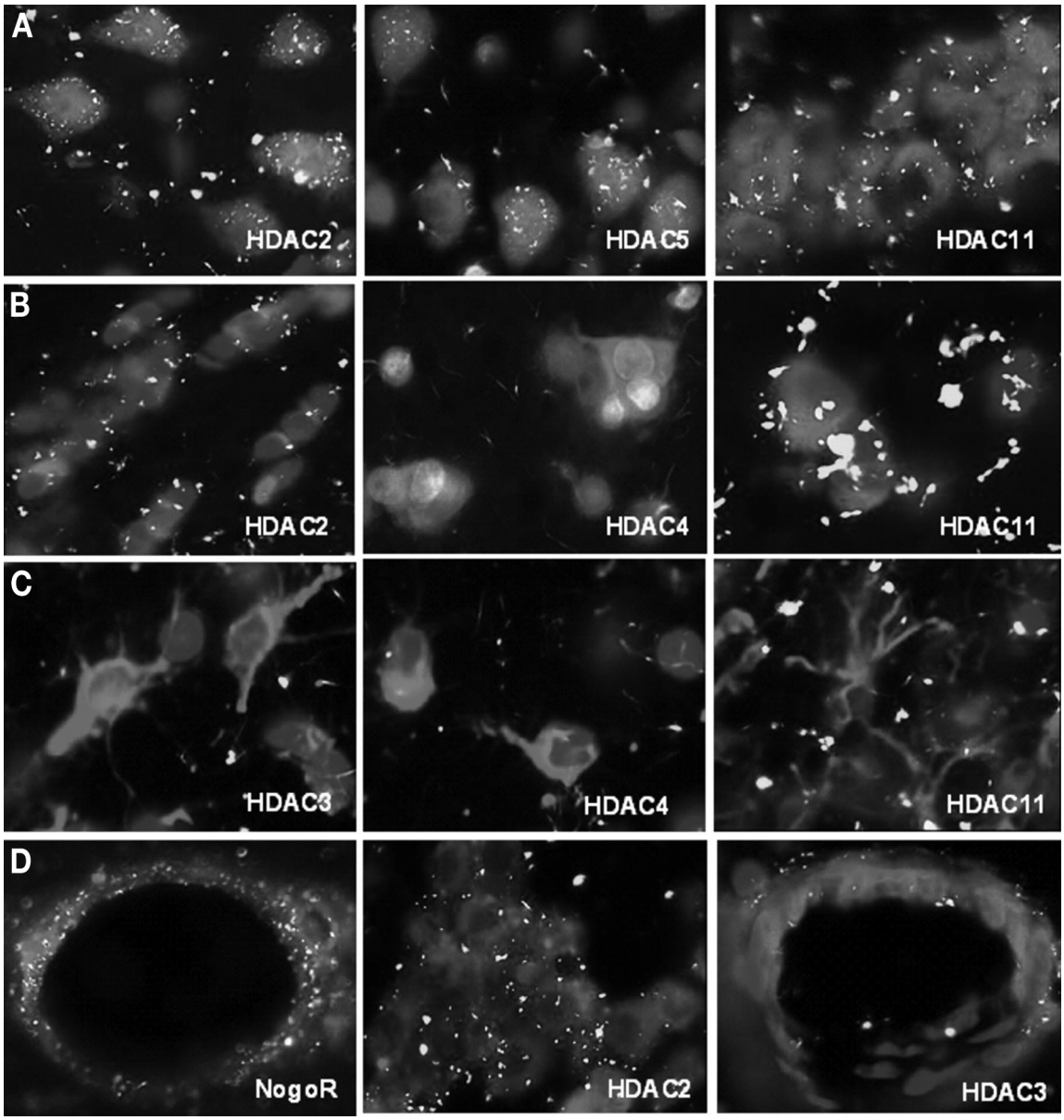

Fig. 5. Double labeling highlights regional and cell type–specific expression of *HDAC* isoforms. Representative photomicrographs showing double labeling for *HDAC* mRNA expression (green, by ISH) and cell type–specific markers (red, by immunohistochemistry). The specific *HDAC* probes used are indicated on each image. Antibodies were used to identify specific cells as follows: **(A)** Anti-*NeuN* was used to label neurons; **(B)** anti-*APC (Ab7)* was used to identify mature oligodendrocytes; **(C)** anti-*GFAP* was used to label astrocytes; **(D)** anti-Von Willibrand factor was used to label vessel endothelial cells. The mouse anti-*CD11*b/c was used to label microglia; however, the signal obtained was not sufficiently above background levels for imaging (data not shown). As a control, Nogo receptor mRNA expression is shown in vessel endothelial cells (*NogoR*). Qualitative analysis was performed on all images as described. Cell nuclei are labeled by DAPI (blue).

The acetylation of nonhistone proteins recently has been observed and suggests a more complex role for the regulation of signal transduction by acetylation and deacetylation. In particular, the activity of *p53* (Vaghefi and Neet, 2004), *Bcl-6* (Bereshchenko et al., 2002), *HSP90* (Yu et al., 2002), and tubulin (Haggarty et al., 2003) are regulated by acetylation. A better understanding of these interactions is clearly important and will enable identification of additional pathways regulated by *HDAC*s. It will be vital to

Table 2
HDAC Isoforms Are Differentially Expressed Among Cell Types in Rat Brain

		HDAC 1	HDAC 2	HDAC 3	HDAC 4	HDAC 5	HDAC 6	HDAC 7	HDAC 8	HDAC 9	HDAC 10	HDAC 11
Neurons	NeuN	~	**	**	**	**	~	~	~	~	*	**
Oligodendrocytes	APC	~	*	*	*	*	~	~	~	~	~	*
Astrocytes	GFAP			~	~	~	~	~	~	~	~	~
Vessel endothelial cells	VW	~	~	~	~	~	~	~	~	~	~	~

Qualitative analysis of double-labeled materials is shown. ~ indicates no expression detected above background; * indicates modest signal detected in some cells; ** indicates signal detected in multiple cells throughout several sections.

consider the role of *HDAC* activity in the context of histone and nonhistone substrates in developing *HDAC* modulators for the CNS.

Some data have pointed to a role of *HDAC* activity in the activation of microglial cells in neurodegeneration as a response to stroke and traumatic brain injury (Ajamian et al., 2003). Although we were not able to detect *HDAC* expression in microglial cells in this set of experiments and in preliminary experiments examining models of stroke (data not presented), this does not exclude the potential involvement of acetylation in microglial activation. This is clearly an area that merits further attention, given recent links between acetylation and neurodegeneration (Ren et al., 2004; Saha and Pahan, 2005). It will also be important to evaluate the potential roles of class-III *HDAC*s (*SIRT1–7*) in the CNS, given recent evidence suggesting the role of *SIRT1* in modulating the neuroprotective effects of NAD in models of axonal degeneration (Araki et al., 2004). These are exciting future studies that should provide more clear roles for class-III *HDAC*s.

The data from this study can focus attention toward regional and cell-specific roles for individual *HDAC* isoforms in the CNS. The use of selective modulators and genetic models will better establish how individual *HDAC*s are functioning in normal and pathological states. This is particularly important for the development of therapeutic agents outside the realm of oncology, such as modulating neurological pathologies and processes. In summary, these studies generated a high-resolution atlas of *HDAC* mRNA expression throughout the rat brain, showing striking regional and subregional expression patterns. Double labeling with cell-specific markers demonstrated that *HDAC* isoforms detected in the brain are expressed primarily in neurons, although some localization of *HDAC* isoforms to oligodendrocytes was observed. Taken together, these data provide a valuable resource for future studies into the role of *HDAC* biology and modulation in the mammalian CNS. This analysis led to an unprecedented level of detail in terms of *HDAC* expression and will contribute to the rational development of the next generation of *HDAC* modulators for neurological indications.

Acknowledgments

This work was supported by Merck & Co.

References

Acharya M. R., Sparreboom A., Venitz J., and Figg W. D. (2005) Rational development of histone deacetylase inhibitors as anticancer agents: a review. *Mol. Pharmacol*. **68,** 917–932.

Ajamian F., Suuronen T., Salminen A., and Reeben M. (2003) Upregulation of class II histone deacetylases mRNA during neural differentiation of cultured rat hippocampal progenitor cells. *Neurosci. Lett*. **346,** 57–60.

Alarcon J. M., Malleret G., Touzani K., et al. (2004) Chromatin acetylation, memory, and LTP are impaired in CBP+/− mice: a model for the cognitive deficit in Rubinstein-Taybi syndrome and its amelioration. *Neuron* **42,** 947–959.

Araki T., Sasaki Y., and Milbrandt J. (2004) Increased nuclear NAD biosynthesis and SIRT1 activation prevent axonal degeneration. *Science* **305,** 1010–1013.

Bereshchenko O. R., Gu W., and Dalla-Favera R. (2002) Acetylation inactivates the transcriptional repressor BCL6. *Nat. Genet*. **32,** 606–613.

Bolger T. A. and Yao T. P. (2005) Intracellular trafficking of histone deacetylase 4 regulates neuronal cell death. *J. Neurosci*. **25,** 9544–9553.

Bradbury C. A., Khanim G. L., Hayden R., et al. (2005) Histone deacetylases in acute myeloid leukaemia show a distinctive pattern of expression that changes selectively in response to deacetylase inhibitors. *Leukemia* **19,** 1751–1759.

Broide R. S., Trembleau A., Ellison J. A., et al. (2004) Standardized quantitative in situ hybridization using radioactive oligonucleotide probes for detecting relative levels of mRNA transcripts verified by real-time PCR. *Brain Res*. **1000,** 211–222.

Camelo S., Iglesias A. H., Hwang D., et al. (2005) Transcriptional therapy with the histone deacetylase inhibitor trichostatin A ameliorates experimental autoimmune encephalomyelitis. *J. Neuroimmunol*. **164,** 10–21.

Chiurazzi P., Pomponi M. G., Pietrobono R., Bakker C. E., Neri G., and Oostra B. A. (1999) Synergistic effect of histone hyperacetylation and DNA demethylation in the reactivation of the FMR1 gene. *Hum. Mol. Genet*. **8,** 2317–2323.

Choi J. H., Oh S. W., Kang M. S., et al. (2001) Expression profile of histone deacetylase 1 in gastric cancer tissues. *Jpn. J. Cancer Res*. **92,** 1300–1304.

Choi J. H., Kwon H. J., Yoon B. I., et al. (2005) Trichostatin A attenuates airway inflammation in mouse asthma model. *Clin. Exp. Allergy* **35,** 89–96.

Dokmanovic M. and Marks P. A. (2005) Prospects: histone deacetylase inhibitors. *J. Cell. Biochem*. **96,** 293–304.

Emerich D. F., Skinner S. J., Borlongan C. V., Vasconcellos A. V., and Thanos C. G. (2005) The choroid plexus in the rise, fall and repair of the brain. *Bioessays* **27,** 262–274.

Ferrante R. J., Kublius J. K., Lee J. et al., (2003) Histone deacetylase inhibition by sodium butyrate chemotherapy ameliorates the neurodegenerative phenotype in Huntington's disease mice. *J. Neurosci*. **23,** 9418–9427.

Franklin K. B. J. and Paxinos G. (1997) *The Mouse Brain in Stereotaxic Coordinates*, Academic Press, San Diego, CA.

Gao L., Cueto M. A., Asselbergs F., and Atadja P. (2002) Cloning and functional characterization of HDAC11, a novel member of the human histone deacetylase family. *J. Biol. Chem*. **277,** 25,748–25,755.

Gardian G., Yang L., Cleren C., Calingasan N. Y., Klivenyi P., and Beal M. F. (2005) Neuroprotective effects of phenylbutyrate in the N171-82Q transgenic mouse model of Huntington's disease. *J. Biol. Chem*. **280,** 556–563.

Gardian G., Browne S. E., Choi D. K., et al. (2004) Neuroprotective effects of phenylbutyrate against MPTP neurotoxicity. *Neuromol. Med*. **5,** 235–241.

Gregoretti I. V., Lee Y. M., and Goodson H. V. (2004) Molecular evolution of the histone deacetylase family: functional implications of phylogenetic analysis. *J. Mol. Biol*. **338,** 17–31.

Haggarty S. J., Koeller K. M., Wong J. C., Grozinger C. M., and Schreiber S. L. (2003) Domain-selective small-molecule inhibitor of histone deacetylase 6 (HDAC6)-mediated tubulin deacetylation. *Proc. Natl. Acad. Sci. U. S. A*. **100,** 4389–4394.

Hao Y., Creson T., Zhang L., et al. (2004) Mood stabilizer valproate promotes ERK pathway-dependent cortical neuronal growth and neurogenesis. *J. Neurosci*. **24,** 6590–6599.

Hockly E., Richon V. M., Woodman B., et al. (2003) Suberoylanilide hydroxamic acid, a histone deacetylase inhibitor, ameliorates motor deficits in a mouse model of Huntington's disease. *Proc. Natl. Acad. Sci. U. S. A*. **100,** 2041–2046.

Hoshino M., Tagawa K., Okuda T., et al. (2003) Histone deacetylase activity is retained in primary neurons expressing mutant huntingtin protein. *J. Neurochem*. **87,** 257–267.

Ito K., Caramori G., Lim S., et al. (2002) Expression and activity of histone deacetylases in human asthmatic airways. *Am. J. Respir. Crit. Care Med*. **166,** 392–396.

Ito K., K., Ito M., Elliott W. M., et al. (2005) Decreased histone deacetylase activity in chronic obstructive pulmonary disease. *N. Engl. J. Med*. **352,** 1967–1976.

Jeong M. R., Hashimoto R., Senatorov V. V. et al., (2003) Valproic acid, a mood stabilizer and anticonvulsant, protects rat cerebral cortical neurons from spontaneous cell death: a role of histone deacetylase inhibition. *FEBS Lett*. **542,** 74–78.

Johnstone R. W. (2002) Histone-deacetylase inhibitors: novel drugs for the treatment of cancer. *Nat. Rev. Drug Discov*. **1,** 287–299.

Kawaguchi Y., Kovacs J. J., McLaruin A., Vance J. M., Ito A., and Yao T. P. (2003) The deacetylase HDAC6 regulates aggresome formation and cell viability in response to misfolded protein stress. *Cell* **115,** 727–738.

Kelly W. K., O'Connor O. A., Krug L. M., et al. (2005) Phase I study of an oral histone deacetylase inhibitor, suberoylanilide hydroxamic acid, in patients with advanced cancer. *J. Clin. Oncol*. **23,** 3923–3931.

Kouraklis G. and Theocharis S. (2002) Histone deacetylase inhibitors and anticancer therapy. *Curr. Med. Chem. Anti-Cancer Agents* **2,** 477–484.

Langley B., Gensert J. M., Beal M. F., and Ratan R. R. (2005) Remodeling chromatin and stress resistance in the central nervous system: histone deacetylase inhibitors as novel and broadly effective neuroprotective agents. *Curr. Drug Targets CNS Neurol. Disord*. **4,** 41–50.

Lin A. Y. (2005) Histone deacetylase activity and COPD, author reply. *N. Engl. J. Med*. **353,** 528,529.

Marks P. A., Miller T., and Richon V. M. (2003) Histone deacetylases. *Curr. Opin. Pharmacol*. **3,** 344–351.

Marks P. A., Richon V. M., Miller T., and Kelley W. K. (2004) Histone deacetylase inhibitors. *Adv. Cancer Res*. **91,** 137–168.

Moradei O., Maroun C. R., Paquin I., and Vaisburg A. (2005) Histone deacetylase inhibitors: latest developments, trends and prospects. *Curr. Med. Chem. Anti-Cancer Agents* **5,** 529–560.

Naruse Y., Oh-hashi K., Iijima N., Naruse M., Yoshioka H., and Tanaka M. (2004) Circadian and light-induced transcription of clock gene Per1 depends on histone acetylation and deacetylation. *Mol. Cell. Biol*. **24,** 6278–6287.

Panteleeva I., Rouaux C., Larmet Y, Boutillier S., Loeffler J. P., and Boutillier A. L. (2004) HDAC-3 participates in the repression of e2f-dependent gene transcription in primary differentiated neurons. *Ann. N. Y. Acad. Sci*. **1030,** 656–660.

Ren M., Leng Y., Jeong M., Leeds P. R., and Chuang D. M. (2004) Valproic acid reduces brain damage induced by transient focal cerebral ischemia in rats: potential roles of histone deacetylase inhibition and heat shock protein induction. *J. Neurochem*. **89,** 1358–1367.

Richon V. M., Zhou X., Rifkind R. A., and Marks P. A. (2001) Histone deacetylase inhibitors: development of suberoylanilide hydroxamic acid (SAHA) for the treatment of cancers. *Blood Cells Mol. Dis*. **27,** 260–264.

Robyr D., Suka Y., Xenarios I., et al. (2002) Microarray deacetylation maps determine genome-wide functions for yeast histone deacetylases. *Cell* **109,** 437–446.

Roth S. Y., Denu J. M., and Allis C. D. (2001) Histone acetyltransferases. *Annu. Rev. Biochem*. **70,** 81–120.

Saha R. N. and Pahan K. (2005) HATs and HDACs in neurodegeneration: a tale of disconcerted acetylation homeostasis. *Cell Death Differ* **39,** 539–550.

Shabbeer S. and Carducci M. A. (2005) Focus on deacetylation for therapeutic benefit. *Investigational Drugs* **8,** 144–154.

Shen S., Li J., and Casaccia-Bonnefil P. (2005) Histone modifications affect timing of oligodendrocyte progenitor differentiation in the developing rat brain. *J. Cell Biol*. **169,** 577–589.

Vaghefi H. and Neet K. E. (2004) Deacetylation of p53 after nerve growth factor treatment in PC12 cells as a post-translational modification mechanism of neurotrophin-induced tumor suppressor activation. *Oncogene* **23,** 8078–8087.

Voelter-Mahlknecht S., Ho A. D., and Mahlknecht U. (2005) Chromosomal organization and localization of the novel class IV human histone deacetylase 11 gene. *Int. J. Mol. Med*. **16,** 589–598.

Yamaguchi M., Tonou-Fujimori N., Komori A., et al. (2005) Histone deacetylase 1 regulates retinal neurogenesis in zebrafish by suppressing Wnt and Notch signaling pathways. *Development* **132,** 3027–3043.

Yu X., Guo Z. S., Marcu M. G., et al. (2002) Modulation of p53, ErbB1, ErbB2, and Raf-1 expression in lung cancer cells by depsipeptide FR901228. *J. Natl. Cancer Inst*. **94,** 504–513.

	Locuslink ID	Unigene	Genbank Seqs
HDAC1	84576	Rn.1863	XM_346065 XP_346066
HDAC2	84577	Rn.1797	XM_342149 XP_342150
HDAC3	84578	Rn.17284	NM_053448 NP_445900
HDAC4	84579	Rn.23483	AF321132 AAK11185
HDAC5	84580	Rn.79863	XM_213469 XP_213469
HDAC6	84581	Rn.13453	XM_228753 XP_228753
HDAC7	84582	Rn.92342	XM_345868 XP_345869
HDAC8	N/A	Rn.23645	XM_343804 XP_343805
HDAC9	314040	N/A	XM_234063 XP_234063
HDAC10	362981	Rn.103671	XM_343311 XP_343312
HDAC11	362400	Rn.100309	XM_342722 XP_342723

Supplemental Methods: Data Analysis

Qualitiative analysis of relative hybridization signal intensity for each *HDAC* isoform was performed on autoradiographic images. More than 50 individual brain regions were examined and scored on a scale of low to high (0–5) intensity. For each brain region, the signal intensity between the different isoforms was compared in relation to the radioactive standards on each film. Global expression levels were calculated as the sum of regional expression values, and an overall rank order of expression was generated. Double-labeling ISH/immunohistochemical analysis was performed for each *HDAC* isoform in association with the different cell markers. Criteria for positively double-labeled cells involved the presence of specific ELF labeling (green), along with cell type–specific labeling (red) and in the presence of a DAPI-labeled nucleus (blue).